Supramolecular interactions lead to remarkably high thermal conductivities in interpenetrated two-dimensional porous crystals

Connor Jaymes Dionne,[†] Muhammad Akif Rahman,[†] Patrick E. Hopkins,[*,‡,¶,§] and Ashutosh Giri[*,†]

†*Department of Mechanical, Industrial and Systems Engineering, University of Rhode Island, Kingston, RI 02881, USA*

‡*Department of Mechanical and Aerospace Engineering, University of Virginia, Charlottesville, Virginia 22904, USA*

¶*Department of Materials Science and Engineering, University of Virginia, Charlottesville, Virginia 22904, USA*

§*Department of Physics, University of Virginia, Charlottesville, Virginia 22904, USA*

E-mail: phopkins@virginia.edu; ashgiri@uri.edu

Abstract

The design of innovative porous crystals with high porosities and large surface areas has garnered a great deal of attention over the past few decades due to their remarkable potential for a variety of applications. However, heat dissipation is key to realizing their potential. We use systematic atomistic simulations to reveal that interpenetrated porous crystals formed from two-dimensional (2D) frameworks possess remarkable thermal conductivities at high porosities in comparison to their three-dimensional (3D) single framework and interpenetrated 3D framework counterparts. In contrast to conventional understanding, higher thermal conductivities are associated with lower atomic densities and higher porosities for porous crystals formed

from interpenetrating 2D frameworks. We attribute this to lower phonon-phonon scattering and vibrational hardening from the supramolecular interactions that restrict atomic vibrational amplitudes, facilitating heat conduction. This marks a new regime of materials design combining ultralow mass densities and ultrahigh thermal conductivities in 2D interpenetrated porous crystals.

Keywords: Metallic organic frameworks, porous crystals, phonon hardening, ultralow mass density, ultra high thermal conductivity

The wide range of structural design through adjustment of linker geometry, length and functional group in metal-organic frameworks (MOFs) and covalent-organic frameworks (COFs) make them one of the most highly sought after materials for targeted applications.[1] Interpenetration or the entwining of multiple lattices in these framework materials not only gives rise to fascinating and intricate architectures but also has been leveraged to improve their physical properties and functionalities.[2–5] For example, the nonbonded, supramolecular interactions (such as van der Waals forces) between the individual networks endows interpenetrated MOFs (IMOFs) with enhanced stability, added structural flexibility and higher gas-adsorption selectivity as compared to single MOFs.[6,7]

The possibility of interpenetration in porous framework materials originates from the large solvent accessible voids that allows for controllable entanglement between the single frameworks. In this regard, predictions from atomistic simulations have been used to identify candidate framework structures with high likelihood of interpenetration.[8–10] Experimentally, chemists have been successful in controlling the degree of interpenetration as well as in gaining unprecedented control over the modulation in the pore volume space in porous framework materials through the manipulation of external conditions such as choosing the appropriate solvents with the desired molecular structures or by changing the reaction temperature.[11–16] For instance, IMOFs with interweaving structures, minimal interpenetration and remarkably large pores ($\sim$1.6 nm) were fabricated by linking symmetrical secondary building units.[17] Whereas, on the other extreme, highly entangled systems with a record 54 interpenetrating networks have also been hydrothermally synthesized.[18]

Therefore, crucial for their incorporation in the applications such as in gas storage, catalysis, electrodes for supercapacitors and energy storage devices is the complete understanding of the influence of interpenetration of porous frameworks on their thermal transport efficiencies.

Recently, thermal transport properties of porous framework materials have been of interest from a materials science standpoint as well as from an applied perspective.[19–26] Most of these works report glass-like thermal conductivities ($\sim$0.3 to 1 W m^{-1} K^{-1}) for porous framework materials, which can be further reduced via pore filling and infiltration of guest species through vibrational scattering mechanisms.[19,24,27] Recently, Sezginel *et al.*[26] have shown that interpenetration of 3D MOF with another guest 3D MOFs can lead to $\sim 2\times$ increase in the thermal conductivity of IMOF structure. They conclude that additional channels of thermal transport introduced through the interpenetration leads to a $2\times$ increase in thermal conductivity of their IMOFs, which can be predicted by a linear sum of the thermal conductivities of the two constituent 3D MOFs. This might be expected in view of the fact that the interpenetration leads to a reduction in porosity and a $2\times$ increase in mass density (that generally results in a concomitant increase in heat conduction in solids).[28,29]

In this work, we show that 3D networks formed from 2D layered frameworks possess thermal conductivities that are more than an order of magnitude higher as compared to a single 3D framework at similar mass densities and are also higher in comparison to 3D interpenetrated frameworks (formed from two individual 3D frameworks with $2\times$ reduced porosities). We show that the massive increase in thermal conductivity holds for a variety of idealized interpenetrated frameworks with a wide range of interatomic interaction parameters that result in stable structures with low densities. This is counterintuitive to the general notion that increased atomic densities lead to higher thermal conductivities in nonmetallic solids. We mostly attribute this to phonon hardening in the interpenetrated frameworks due to the supramolecular interactions between the 2D layers that restricts the motion of the atoms. We apply our proof of concept to a realistic framework that is designed based on the 2D COF-1 structure. Our results show that these interpenetrated frameworks can possess more than an order of magnitude higher thermal conductivity compared

to the prototypical 3D COF-300 structure at similar mass densities and porosities. This highlights the prowess of interpenetrated frameworks made from 2D layers as structural materials with ultralight weight characteristics accompanied by superior thermal transport properties that separate them from any other class of materials.

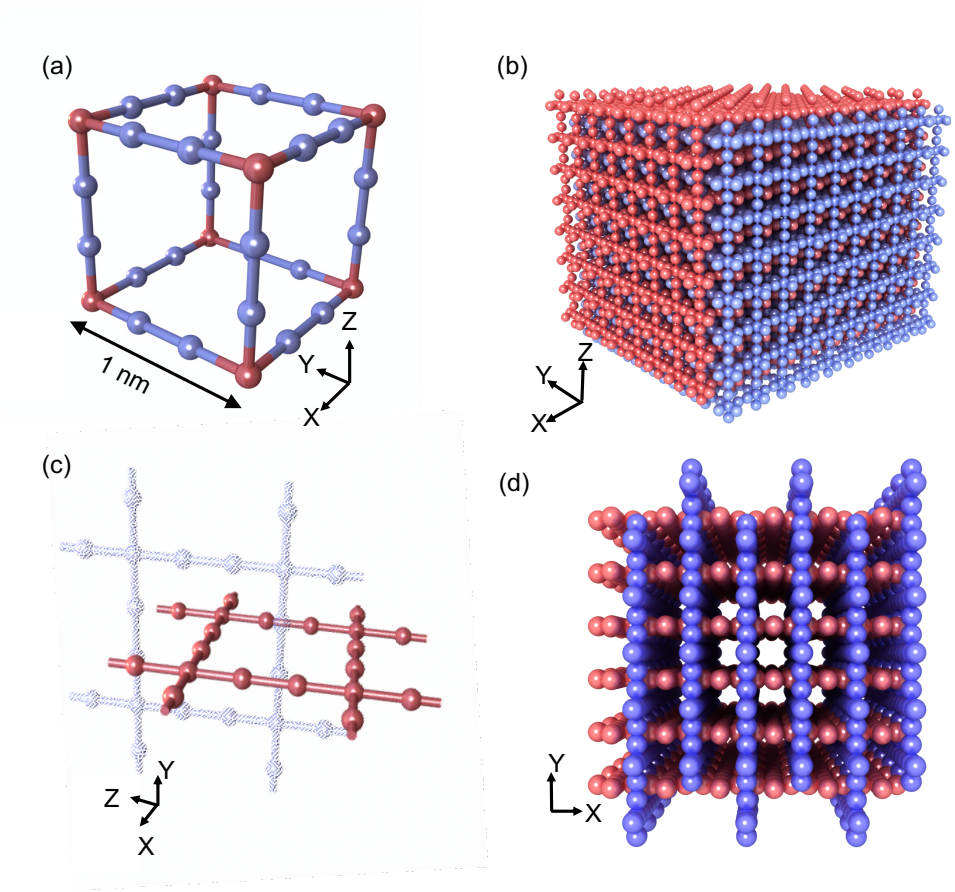

Figure 1: (a) Schematic illustration of the unit cell for our 3D idealized porous crystals. (b) The atoms are displaced by 5 Å in all three principle directions to form an interpenetrated 3D porous crystal as shown in the schematic of the 2D→3D. (c) Similarly, our interpenetrated 2D→3D structures are formed by interpenetrating 2D orthogonal layers. (d) Schematic cross-sectional view of our computational domain for the interpenetrated 2D→3D idealized porous crystals. We use computational domain sizes of $80 \times 80 \times 80$ Å^3 for all our structures.

To systematically investigate the effect of varying interactions between the single frameworks, we perform atomistic simulations on idealized porous structures as opposed to realistic materials since we are more interested in the qualitative insight on the effect of interpenetration of 2D layered frameworks on thermal transport as opposed to their material specific properties. Figure 1a

shows our idealized cubic structure with a pore volume of $\sim$ 1 nm^3. Similar idealized structures have been used to glean significant insight into the thermal transport properties of MOFs.[19,23,26] Our interpenetrated structures based on 3D (Fig. 1b) and 2D (Fig. 1c) frameworks are generated by creating copies and translating the idealized structures. An example of the computational domain formed through interpenetration of idealized 2D frameworks (2D$\rightarrow$3D) is shown in Fig. 1d. We base the interatomic potential for our idealized crystals on the COMPASS force field[30], with the nonbonded interactions between interpenetrating frameworks defined by a Lennard-Jones (LJ) potential, $V(r) = \varepsilon[2(\sigma/r)^9 - 3(\sigma/r)^6]$, where r is the interatomic separation, and σ and ε are the LJ length and energy parameters, respectively. A range of σ and ε values are chosen to understand the effect of interframework interactions; as the value of σ determines an individual frameworks' mobility, we can systematically control the positioning of the frameworks relative to each other in our interpenetrated structures (see Supporting Information for details regarding the force field parameters). We note that depending on the linker shape and size, the porosity and the van der Waals dimension (that would fit in the pores without touching the pore walls) can be methodically varied in realistic framework materials.[31] For example, in the isorecticular MOF series, depending on the size of the ligands controlled through pore functionalization, the percent free volume in the crystals can be systematically varied from $\sim$56 % to 91 %.[31] For interpenetrated structures, this also allows for the control of an individual frameworks' mobility.[26]

Figure 2a shows the thermal conductivities of our idealized structures as a function temperature, which are calculated based on the Green-Kubo (GK) approach. (see Supporting information for more details). Also shown are the respective $1/T$ fits highlighting the strong role of anharmonic Umklapp scattering processes in all of our structures.[32,33] The more notable result shown in Fig. 2a is the dramatic increase in thermal conductivity (by almost an order of magnitude) of the structure formed from the interpenetration of 2D frameworks into a single 3D framework (2D$\rightarrow$3D). This is much higher in comparison to the two fold increase in thermal conductivity of the structure formed by the interpenetration of 3D frameworks (3D$\rightarrow$3D) as shown in the figure. It is also interesting to note that while the density of the 3D$\rightarrow$3D interpenetration is twice as high as the

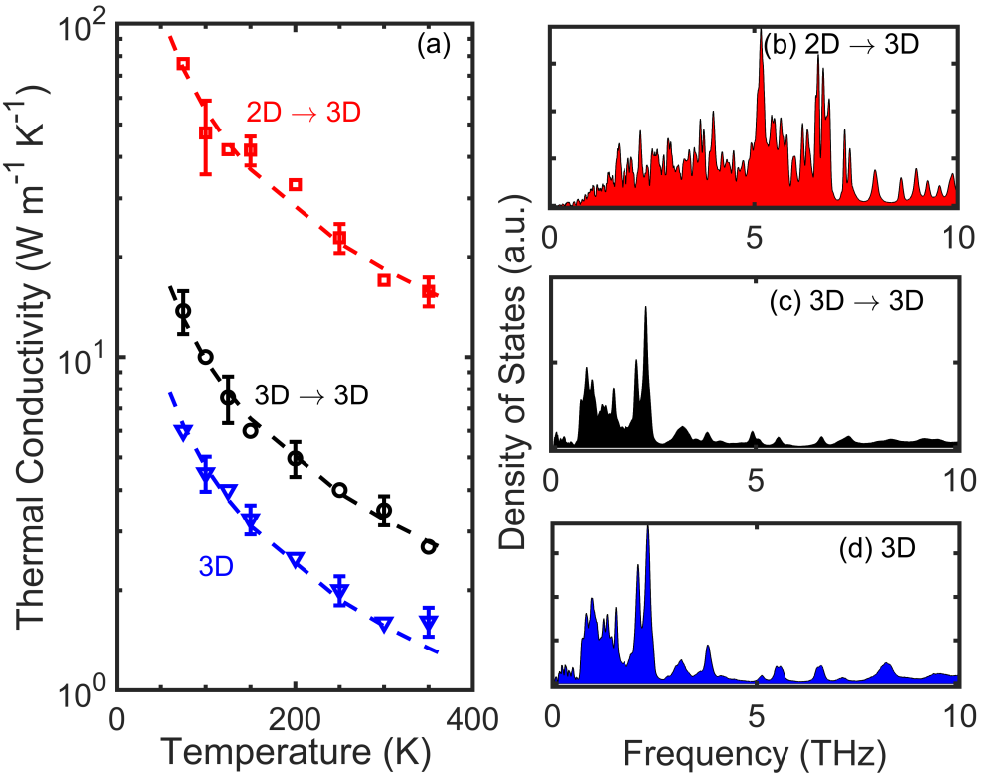

Figure 2: (a) Temperature dependent thermal conductivities of our idealized 3D, interpenetrated 2D→3D and interpenetrated 3D→3D porous crystals. The dashed lines represent the $1/T$ temperature trends highlighting the role of anharmonic phonon-phonon scattering in these idealized structures. The interpenetrated 2D→3D structure shows drastically enhanced thermal conductivities throughout the temperature range in comparison to both the 3D and the interpenetrated 3D→3D structures; although the mass density of the interpenetrated 3D→3D structure is twice that of the 3D case, our interpenetrated 2D→3D has a similar low mass density as that of the 3D structure all the while possessing an order of magnitude higher thermal conductivity. Vibrational density of states of our (b) interpenetrated 2D→3D, (c) interpenetrated 3D→3D and (d) 3D structures calculated from molecular dynamics simulations.

single 3D framework, the density of the 2D→3D structure is comparable to that of the individual 3D framework; for crystalline solids in general, an increase in density is usually accompanied by an enhancement in their thermal and mechanical properties.[34] This suggests that the mechanism behind the dramatic increase in heat conduction in our 2D→3D frameworks could be different in comparison to the 3D→3D case, where it has been previously shown by Sezginel *et al.*[26] that additional channels of heat transfer are introduced by the interpenetration of two 3D frameworks.

To understand the mechanism leading to the dramatic thermal conductivity increase in our 2D→3D structures, we first compare the vibrational density of states (DOS) of our frameworks as shown in Figs. 2b-d. The DOS for the 3D and 3D→3D cases are similar, while the DOS for the 2D→3D shows pronounced phonon hardening as compared to the other two cases. Moreover, the heat carrying vibrations (as predicted by the spectral heat flux calculations detailed in the Supporting Information) in the 3D and 3D→3D cases are also similar, reinforcing the suggestion that additional heat transfer pathways are introduced in the same frequency range due to interpenetration of two 3D frameworks without affecting the spectral nature (see Fig. S6). In contrast, spectral heat flux calculations show that heat carrying vibrations in the 2D→3D case encompasses a broader spectral range (see Figs. 2b-d). Normalizing the frequency range for our structures and calculating the per mode contribution to the total heat flux shows that in the 2D→3D case, the proportion of heat carrying vibrations are shifted to comparatively higher frequencies (in a per-mode-basis).

From the above discussion, we observe that vibrational hardening can lead to a significantly enhanced thermal conductivity in interpenetrated structures formed by 2D frameworks. The effect on thermal conductivity of interframework interactions between the interpenetrated 2D layers, however, needs to be fully understood in order to design frameworks with superior thermal transport properties. Therefore, we investigate the changes in the thermal conductivity, mean squared displacement (MSD) and density for our 2D→3D structures across a wide range of values of ε and σ (see Figure 3). As shown by the darker shaded regions in Fig. 3a, even though a high value of ε represents better coupling between the frameworks, it does not guarantee a high thermal conductivity since the value of σ also affects thermal transport in our interpenetrated structures; σ can

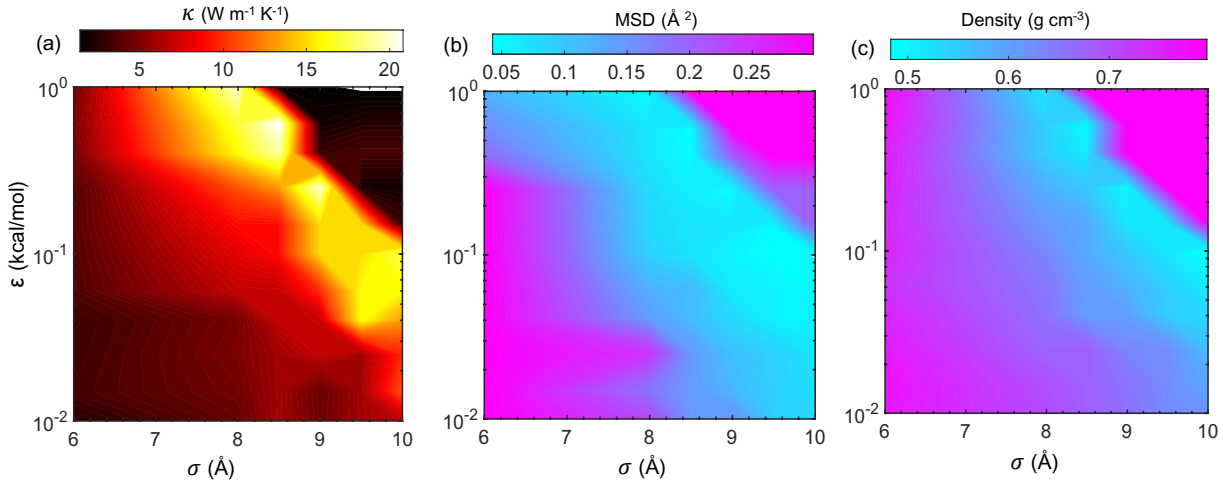

Figure 3: Effect of framework interaction on (a) thermal conductivity, (b) mean square displacement (MSD) of the atoms, and (c) mass density. The combinations of energy (ε) and length (σ) parameters that result in high thermal conductivities are associated with low mass densities and MSDs of the frameworks. Usually for crystalline solids, higher mass densities are associated with higher thermal conductivities. For interpenetrated 2D$\rightarrow$3D porous crystals, however, the further apart the 2D layers are with respect to each other, the higher the thermal conductivities. Similarly, 2D layers that are "locked-in" demonstrate comparatively higher thermal conductivities, which can be attributed to lower phonon-phonon scattering.

have a major influence on the framework's mobility with a high value allowing structural stability for the 2D frameworks, whereas a low value results in the translation of the 2D layers relative to each other as demonstrated in Fig. 3b. Comparing Figs. 3a and 3b, it becomes apparent that a lower MSD (where the frameworks are more likely to be "locked in" their equilibrium positions) leads to higher thermal conductivities.

The values of ε and σ can also affect the mechanical properties and structural integrity of the 2D$\rightarrow$3D interpenetrated frameworks. As shown in Fig. 3c, lower densities are associated with similar combinations of the force field parameters that also lead to higher thermal conductivities (Fig. 3a). As noted above, this is contrary to the general understanding of crystalline solids where higher densities usually lead to higher thermal conductivities.[34] For these 2D interpenetrated structures, the combination of force field parameters that result in lower densities also lead to higher Young's modulus and higher stress response as calculated from additional simulations of uniaxial tension on the interpenetrated frameworks (see Fig. S9). We note that as higher Young's modulus is generally associated with higher sound velocity in solids, the increasing Young's modulus is also indicative of higher velocities for Debye-like phonons in the interpenetrated structures with the combination of force field parameters that result in higher thermal conductivities.

Finally, to show that our results are applicable for realistic organic-based framework materials, we design 2D$\rightarrow$3D interpenetrated frameworks by orthogonally combining 2D layers based on the COF-1 structures as shown in the schematic of the computational domain in Fig. 4a. Along with the parameters for the Polymer consistent force-field describing the interatomic interactions, the schematic of the unit cell of our COF-1 structure are given in the Supporting Informations. We note that there have been several similar 3D networks generated from 2D layers reported in prior literature.[2,35–41] For comparison, we also calculate the thermal conductivity for a 3D COF-300 structure with a similar mass density (the schematic of the domain is shown in Fig. 4b). Figure 4c shows the temperature dependent thermal conductivities of the two structures highlighting the more than an order of magnitude higher thermal conductivity of our 2D$\rightarrow$3D structure based on COF-1. Moreover, the interpenetrated framework also shows a more pronounced $1/T$ trend

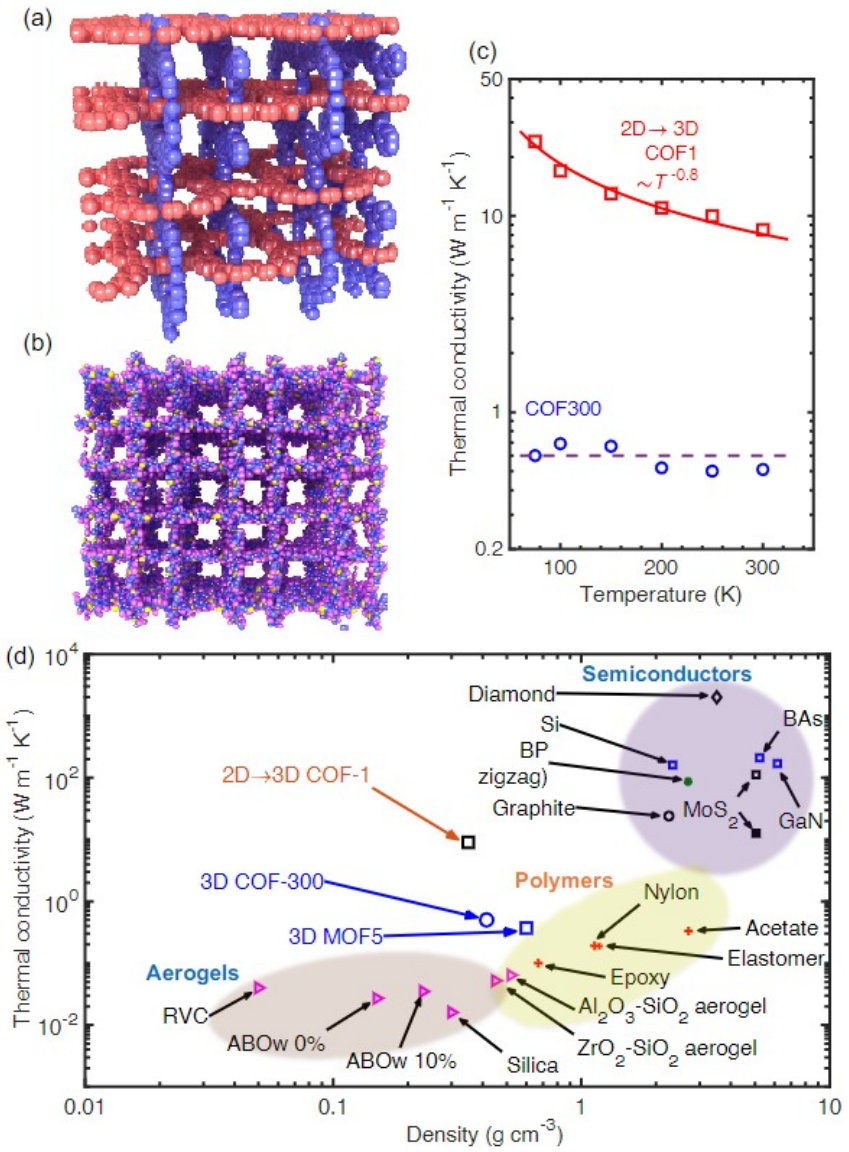

Figure 4: Schematic representations of our (a) interpenetrated 2D→3D porous framework based on the realistic material COF-1 and (b) 3D porous crystal based on COF-300. (c) The thermal conductivity of the interpenetrated structure is remarkably higher in comparison to the 3D counterpart even though the mass densities are similar for the two structures. The temperature dependence (or the lack thereof for the 3D COF-300) structure suggests that vibrational scattering at the pore walls dictates thermal conductivity in the 3D COF-300 case, whereas anharmonic phonon scattering is more dominant in the interpenetrated structure. (d) Thermal conductivity as a function of mass density for different classes of materials. Semiconductors with relatively higher mass densities have higher thermal conductivities, whereas porous solids such as metal organic frameworks, covalent organic frameworks and aerogels possess low thermal conductivities. Our interpenetrated 2D→3D structure based on COF-1 marks a new regime of materials design combining ultralow densities and ultrahigh thermal conductivities.

(see Fig. 4c) compared to 3D COF-300, which is usually attributed to Umklapp scattering or anharmonic phonon-phonon scattering dominated processes dictating heat conduction. For defect free, crystalline solids these multiple phonon scattering processes create thermal resistance and lead to the typical $1/T$ trend with temperature.[32,33] In contrast to our COF-1 based interpenetrated framework, the thermal conductivity for our COF-300 structure is independent of temperature for the temperature range studied in this work, which can mostly be attributed to vibrational scattering at the pore walls in the 3D structure.

To gauge the thermal performance of our 2D$\rightarrow$3D interpenetrated frameworks, we compare the thermal conductivity of our interpenetrated COF-1 structure with that of other classes of materials as a function of their mass densities in Fig. 4c. In general, the increase in mass density usually leads to higher thermal conductivities as exemplified by the relatively higher thermal conductivities for metals and semiconductors. Similarly, fully dense 2D materials such as BP and MoS_2 also possess high thermal conductivities. The thermal conductivity of MOF-5 and COF-300 show enhanced thermal conductivity compared to aerogels and other porous materials with similar mass densities. However, our interpenetrated COF-1 structure with more than a ten-fold increase in thermal conductivity compared to the 3D organic frameworks marks a new regime of materials design that combines ultrahigh thermal conductivity with ultralow mass density. This regime can particularly be useful for structural materials that demand superior physical properties such as high thermal conductivity.[42,43]

In summary, our systematic atomistic simulations show that porous framework solids made from the interpenetration of 2D layers are endowed with enhanced thermal transport properties that derive from the supramolecular interactions between the frameworks. We show that interpentration of 2D layers have superior thermal conductivities as compared to individual and interpenetrated 3D frameworks. We ascribe this to the enhanced phonon hardening and shift of heat carrying vibrations to higher frequencies in the interpenetrated 2D porous crystals. In contrast to the conventional understanding, our results from extensive MD simulations show that for interpenetrated 2D frameworks, high thermal conductivities are associated with higher porosities. With the

growing interest for organic framework materials, 2D→3D interpenetration in COFs and MOFs paves a new strategy in attaining "user-defined" physical properties in these materials through control over the level of interpenetration between the individual 2D layers. These physical properties could potentially be further manipulated by the introduction of guest molecules inside the pores. In this regard, our interpenetration scheme could also increase gas storage capacities by increasing adsorption sites and also leading to better thermal management of the large amounts of heat generated during adsorption.

Acknowledgement

This manuscript is based upon work supported by the Office of Naval Research, Grant No.'s N00014-21-1-2622 and N00014-20-1-2686. The work is also partially supported by the National Science Foundation (NSF Award No. 2119365).

Competing Interests

The authors declare no competing interests.

Data Availability

The data supporting the present work is available from the corresponding authors upon reasonable request

Supporting Information Available

The Supporting information is available free of charge at .

- Details of the computational domain setup, equilibrium molecular dynamics approach, non-equilibrium molecular dynamics approach, interatomic potentials, spectral heat flux, me-

chanical properties.

References

(1) Lu, W.; Wei, Z.; Gu, Z.-Y.; Liu, T.-F.; Park, J.; Park, J.; Tian, J.; Zhang, M.; Zhang, Q.; Gentle III, T.; Bosch, M.; Zhou, H.-C. Tuning the structure and function of metal–organic frameworks via linker design. *Chem. Soc. Rev.* **2014**, *43*, 5561–5593.

(2) Chakraborty, G.; Park, I.-H.; Medishetty, R.; Vittal, J. J. Two-Dimensional Metal-Organic Framework Materials: Synthesis, Structures, Properties and Applications. *Chemical Reviews* **2021**, *121*, 3751–3891.

(3) Jiang, H.-L.; Makal, T. A.; Zhou, H.-C. Interpenetration control in metal–organic frameworks for functional applications. *Coordination Chemistry Reviews* **2013**, *257*, 2232–2249.

(4) Gong, Y.-N.; Zhong, D.-C.; Lu, T.-B. Interpenetrating metal–organic frameworks. *CrystEngComm* **2016**, *18*, 2596–2606.

(5) Gupta, M.; Vittal, J. J. Control of interpenetration and structural transformations in the interpenetrated MOFs. *Coordination Chemistry Reviews* **2021**, *435*, 213789.

(6) Yang, J.; Hu, T.; Mak, T. C. W. Flexible Bis(imidazole) Mediated Assembly of Silver(I)–Organic Frameworks with Ethynide and Trifluoroacetate Ligands. *Crystal Growth & Design* **2014**, *14*, 2990–3001.

(7) Ma, L.; Lin, W. Unusual Interlocking and Interpenetration Lead to Highly Porous and Robust Metal–Organic Frameworks. *Angewandte Chemie International Edition* **2009**, *48*, 3637–3640.

(8) Kwon, O.; Park, S.; Zhou, H.-C.; Kim, J. Computational prediction of hetero-interpenetration in metal–organic frameworks. *Chem. Commun.* **2017**, *53*, 1953–1956.

(9) Sezginel, K. B.; Feng, T.; Wilmer, C. E. Discovery of hypothetical hetero-interpenetrated MOFs with arbitrarily dissimilar topologies and unit cell shapes. *CrystEngComm* **2017**, *19*, 4497–4504.

(10) Blatov, V. A.; Carlucci, L.; Ciani, G.; Proserpio, D. M. Interpenetrating metal–organic and inorganic 3D networks: a computer-aided systematic investigation. Part I. Analysis of the Cambridge structural database. *CrystEngComm* **2004**, *6*, 377–395.

(11) Rankine, D.; Avellaneda, A.; Hill, M. R.; Doonan, C. J.; Sumby, C. J. Control of framework interpenetration for in situ modified hydroxyl functionalised IRMOFs. *Chem. Commun.* **2012**, *48*, 10328–10330.

(12) Farha, O. K.; Malliakas, C. D.; Kanatzidis, M. G.; Hupp, J. T. Control over Catenation in MetalOrganic Frameworks via Rational Design of the Organic Building Block. *Journal of the American Chemical Society* **2010**, *132*, 950–952.

(13) Reineke, T. M.; Eddaoudi, M.; Moler, D.; O'Keeffe, M.; Yaghi, O. M. Large Free Volume in Maximally Interpenetrating Networks: The Role of Secondary Building Units Exemplified by Tb2(ADB)3[(CH3)2SO]4·16[(CH3)2SO]1. *Journal of the American Chemical Society* **2000**, *122*, 4843–4844.

(14) Long, D.-L.; Hill, R. J.; Blake, A. J.; Champness, N. R.; Hubberstey, P.; Wilson, C.; Schröder, M. Anion Control over Interpenetration and Framework Topology in Coordination Networks Based on Homoleptic Six-Connected Scandium Nodes. *Chemistry – A European Journal* **2005**, *11*, 1384–1391.

(15) Ferguson, A.; Liu, L.; Tapperwijn, S. J.; Perl, D.; Coudert, F.-X.; Van Cleuvenbergen, S.; Verbiest, T.; van der Veen, M. A.; Telfer, S. G. Controlled partial interpenetration in metal–organic frameworks. *Nature Chemistry* **2016**, *8*, 250–257.

(16) Shekhah, O.; Wang, H.; Paradinas, M.; Ocal, C.; Schüpbach, B.; Terfort, A.; Zacher, D.;

Fischer, R. A.; Wöll, C. Controlling interpenetration in metal–organic frameworks by liquid-phase epitaxy. *Nature Materials* **2009**, *8*, 481–484.

(17) Chen, B.; Eddaoudi, M.; Hyde, S. T.; O'Keeffe, M.; Yaghi, O. M. Interwoven Metal-Organic Framework on a Periodic Minimal Surface with Extra-Large Pores. *Science* **2001**, *291*, 1021–1023.

(18) Wu, H.; Yang, J.; Su, Z.-M.; Batten, S. R.; Ma, J.-F. An Exceptional 54-Fold Interpenetrated Coordination Polymer with 103-srs Network Topology. *Journal of the American Chemical Society* **2011**, *133*, 11406–11409.

(19) Babaei, H.; Wilmer, C. E. Mechanisms of Heat Transfer in Porous Crystals Containing Adsorbed Gases: Applications to Metal-Organic Frameworks. *Phys. Rev. Lett.* **2016**, *116*, 025902.

(20) Huang, B. L.; Ni, Z.; Millward, A.; McGaughey, A. J. H.; Uher, C.; Kaviany, M.; Yaghi, O. Thermal conductivity of a metal-organic framework (MOF-5): Part II. Measurement. *International Journal of Heat and Mass Transfer* **2007**, *50*, 405–411.

(21) Talin, A. A.; Jones, R. E.; Hopkins, P. E. Metal–organic frameworks for thermoelectric energy-conversion applications. *MRS Bulletin* **2016**, *41*, 877–882.

(22) Erickson, K. J.; Leonard, F.; Stavila, V.; Foster, M. E.; Spataru, C. D.; Jones, R. E.; Foley, B. M.; Hopkins, P. E.; Allendorf, M. D.; Talin, A. A. Thin Film Thermoelectric Metal-Organic Framework with High Seebeck Coefficient and Low Thermal Conductivity. *Advanced Materials* **2015**, *27*, 3453–3459.

(23) Babaei, H.; McGaughey, A. J. H.; Wilmer, C. E. Effect of pore size and shape on the thermal conductivity of metal-organic frameworks. *Chem. Sci.* **2017**, *8*, 583–589.

(24) Babaei, H.; DeCoster, M. E.; Jeong, M.; Hassan, Z. M.; Islamoglu, T.; Baumgart, H.; McGaughey, A. J. H.; Redel, E.; Farha, O. K.; Hopkins, P. E.; Malen, J. A.; Wilmer, C. E.

Observation of reduced thermal conductivity in a metal-organic framework due to the presence of adsorbates. *Nature Communications* **2020**, *11*, 4010.

(25) Evans, A. M. et al. Thermally conductive ultra-low-k dielectric layers based on two-dimensional covalent organic frameworks. *Nature Materials* **2021**, *20*, 1142–1148.

(26) Sezginel, K. B.; Asinger, P. A.; Babaei, H.; Wilmer, C. E. Thermal Transport in Interpenetrated Metal–Organic Frameworks. *Chemistry of Materials* **2018**, *30*, 2281–2286.

(27) Koza, M. M.; Johnson, M. R.; Viennois, R.; Mutka, H.; Girard, L.; Ravot, D. Breakdown of phonon glass paradigm in La- and Ce-filled Fe4Sb12 skutterudites. *Nature Materials* **2008**, *7*, 805–810.

(28) Slack, G. Nonmetallic crystals with high thermal conductivity. *Journal of Physics and Chemistry of Solids* **1973**, *34*, 321 – 335.

(29) Giri, A.; Hopkins, P. E. Achieving a better heat conductor. *Nature Materials* **2020**, *19*, 482–484.

(30) Sun, H. COMPASS: An ab Initio Force-Field Optimized for Condensed-Phase ApplicationsOverview with Details on Alkane and Benzene Compounds. *The Journal of Physical Chemistry B* **1998**, *102*, 7338–7364.

(31) Eddaoudi, M.; Kim, J.; Rosi, N.; Vodak, D.; Wachter, J.; O'Keeffe, M.; Yaghi, O. M. Systematic Design of Pore Size and Functionality in Isoreticular MOFs and Their Application in Methane Storage. *Science* **2002**, *295*, 469–472.

(32) Klemens, P. G. The scattering of low-frequency lattice waves by static imperfections. *Proceedings of the Physical Society. Section A* **1955**, *68*, 1113–1128.

(33) Kittel, C. *Introduction to Solid State Physics*, 6th ed.; John Wiley & Sons, Inc.: New York, 1986.

(34) Goodson, K. E. Ordering Up the Minimum Thermal Conductivity of Solids. *Science* **2007**, *315*, 342–343.

(35) Xu, N.-N.; Qian, L.-W.; Li, Z.-Q.; Bian, G.-Q.; Zhu, Q.-Y.; Dai, J. An MOF-like Interpenetrated 2D Plus 2D to 3D Inorganic Grid Assembled by Linear Inorganic Pillars, Structures, and Properties in Supercapacitance. *Inorganic Chemistry* **2018**, *57*, 9153–9159.

(36) Carlucci, L.; Ciani, G.; M. Proserpio, D. Three-dimensional architectures of intertwined planar coordination polymers: the first case of interpenetration involving two different bidimensional polymeric motifs. *New J. Chem.* **1998**, *22*, 1319–1321.

(37) Meng, M.; Zhong, D.-C.; Lu, T.-B. Three porous metal–organic frameworks based on an azobenzenetricarboxylate ligand: synthesis, structures, and magnetic properties. *CrystEngComm* **2011**, *13*, 6794–6800.

(38) Gómez-Lor, B.; Gutiérrez-Puebla, E.; Iglesias, M.; Monge, M. A.; Ruiz-Valero, C.; Snejko, N. Novel 2D and 3D Indium Metal-Organic Frameworks: Topology and Catalytic Properties. *Chemistry of Materials* **2005**, *17*, 2568–2573.

(39) Carlucci, L.; Ciani, G.; Proserpio, D. M.; Rizzato, S. New architectures from the self-assembly of MIISO4 salts with bis(4-pyridyl) ligands. The first case of polycatenation involving three distinct sets of 2D polymeric (4,4)-layers parallel to a common axis. *CrystEngComm* **2003**, *5*, 190–199.

(40) Chen, L.; Tan, K.; Lan, Y.-Q.; Li, S.-L.; Shao, K.-Z.; Su, Z.-M. Unusual microporous polycatenane-like metal–organic frameworks for the luminescent sensing of Ln3+ cations and rapid adsorption of iodine. *Chem. Commun.* **2012**, *48*, 5919–5921.

(41) Garai, B.; Shetty, D.; Skorjanc, T.; Gándara, F.; Naleem, N.; Varghese, S.; Sharma, S. K.; Baias, M.; Jagannathan, R.; Olson, M. A.; Kirmizialtin, S.; Trabolsi, A. Taming the Topology of Calix[4]arene-Based 2D-Covalent Organic Frameworks: Interpenetrated vs Noninterpene-

trated Frameworks and Their Selective Removal of Cationic Dyes. *Journal of the American Chemical Society* **2021**, *143*, 3407–3415.

(42) Meza, L. R.; Das, S.; Greer, J. R. Strong, lightweight, and recoverable three-dimensional ceramic nanolattices. *Science* **2014**, *345*, 1322–1326.

(43) Giri, A.; Tomko, J.; Gaskins, J. T.; Hopkins, P. E. Large tunability in the mechanical and thermal properties of carbon nanotube-fullerene hierarchical monoliths. *Nanoscale* **2018**, *10*, 22166–22172.

TOC Graphic